

Dynamic Spin Correlation Function near the Antiferromagnetic Quantum Phase Transition of Heavy-Fermions

C. Pépin¹ and M. Lavagna²

*Commissariat à l'Energie Atomique,
Département de Recherche Fondamentale sur la Matière Condensée/SPSMS,
17, rue des Martyrs,
38054 Grenoble Cedex 9, France*

The dynamical spin susceptibility is studied in the magnetically-disordered phase of heavy-Fermion systems near the antiferromagnetic quantum phase transition. In the framework of the $S = 1/2$ Kondo lattice model, we introduce a perturbative expansion treating the spin and Kondo-like degrees of freedom on an equal footing. The dynamical spin susceptibility displays a two-component behaviour in agreement with the inelastic neutron scattering (INS) experiments performed in $CeCu_6$, $Ce_{1-x}La_xRu_2Si_2$ and UPt_3 : a quasielastic q -independent peak as in a Fermi liquid theory, and a strongly q -dependent inelastic peak typical of a non-Fermi liquid behaviour. Very strikingly, the position of the inelastic peak is found to be pushed to zero at the antiferromagnetic transition. The picture is consistent with the neutron cross sections observed in INS experiments.

PACS numbers: 71.27.+a, 75.20.Hr, 75.40.Gb

I. INTRODUCTION

One of the most striking properties of heavy Fermion compounds discovered these last years is the existence of a quantum phase transition [1,2] driven by composition change (at $x_C = 0.1$ in $CeCu_{6-x}Au_x$ and $x_C = 0.08$ in $Ce_{1-x}La_xRu_2Si_2$), pressure or magnetic field. It has been largely discussed in various theoretical approaches [5,6]. Important insight is provided by the evolution of the low temperature neutron cross section measured by Inelastic Neutron Scattering (INS) experiments when getting closer to the magnetic instability. The experiments performed in pure compounds $CeCu_6$ and $CeRu_2Si_2$ by Regnault et al [3] and Aeppli et al [4] have shown the presence of two distinct contributions to the dynamic magnetic structure factor: a q -independent quasielastic component, and a strongly q -dependent inelastic peak with a maximum at the value ω_{\max} of the frequency. The former corresponds to localized excitations of Kondo-type while the latter peaked at some wavevector Q is believed to be associated with intersite magnetic correlations due to RKKY interactions. The frequency-width of the quasielastic and inelastic peaks respectively define the single-site and intersite relaxation rate Γ_{SS} and Γ_{IS} . Such features have also been observed in UPt_3 and called as "slow" and "fast" components by Bernhoeft and Lonzarich [7]. Later on, INS experiments have been performed with varying compositions as in $Ce_{1-x}La_xRu_2Si_2$ [8]. It has been observed a narrowing of the single-site relaxation rate Γ_{SS} when getting closer to the magnetic transition. At the same time, both the position of the inelastic peak ω_{\max} and the intersite relaxation rate Γ_{IS} drastically decrease when getting near the magnetic instability. Table 1 reports the values of Γ_{SS} , Γ_{IS} and ω_{\max} for the different compounds.

Any theory aimed to describe the quantum critical phenomena in heavy-Fermion compounds should account for the so-quoted behaviour of the dynamical spin susceptibility. We start from the Kondo lattice model which is believed to describe the physics of these systems. We refer to the recent paper of Tsunetsugu et al [9] for a review of the model. As already pointed out by Doniach in his initial paper [10], the main features result of the competition between the Kondo effect and the RKKY interactions among spins mediated by the conduction electrons. Most of the theories developed so far [11–15] agree with the existence of a hybridization gap which splits the Abrikosov-Suhl or Kondo resonance formed at the Fermi level. The role of the interband transitions has been outlined for long in order to explain the inelastic component of the dynamical spin susceptibility. For instance, the theories based on a $1/N$ expansion [16–20] (where N is simultaneously the degeneracy of the conduction electrons and of the spin channels) predict a maximum of $\chi''(k_F, \omega)/\omega$ at ω_{\max} of the order of the indirect hybridization gap [21]. However, the $1/N$ expansion theories present serious drawbacks: (i) the spin fluctuation effects are automatically ruled out since the RKKY interactions only occur at the following order in $1/N^2$ [22], (ii) they then fail to describe any magnetic instability and hence the quantum critical phenomena mentioned above and (iii) the predictions for ω_{\max} and the associated relaxation rate cannot account for the experimental observations near the

magnetic instability. An improvement brought by Doniach [23] consists to consider the $1/N^2$ corrections in an instantaneous approximation: it gives back the ladder diagram contribution to the dynamical spin susceptibility and then accounts for the spin fluctuation effects. Other approaches were proposed in Ref. [24–26]. But still the predictions for the frequency dependence of the dynamic magnetic structure factor presents a gap of the order of the hybridization gap whatever the value of the interaction is. On the other hand, in front of the difficulties encountered when starting from microscopic descriptions, various phenomenological models (as the duality model of Kuramoto and Miyake [27] and reference [7]) have been introduced to describe both the spin fluctuation and the itinerant electron aspects with some successful predictions as the weak antiferromagnetism of these systems.

In this paper, we develop a systematic approach to the Kondo lattice model for $S = 1/2$ ($N = 2$) in which the Kondo-like and the spin degrees of freedom are treated on an equal footing. The presented approach shows some similarities with earlier works [11,15]. But while Ref. [11,15] essentially describe the phase diagram of the Kondo lattice at a mean-field level, we focus on the effects of spin fluctuations in the magnetically-disordered phase hence bringing the spin-fluctuation and the Kondo effect theories together. The saddle-point results and the gaussian fluctuations in the charge channel are consistent with the standard $1/N$ theories. In addition, the gaussian fluctuations in the spin channel restore the spin fluctuation effects which were missing in the $1/N$ expansion. The general expression of the dynamical spin susceptibility that we derive reproduces some of the features postulated in the phenomenological models. It presents a two-component behaviour: a quasielastic component superimposed on an inelastic peak with renormalized values of the relaxation rates, susceptibilities and ω_{\max} . In a very striking way, ω_{\max} is pushed to zero and the inelastic mode becomes soft at the antiferromagnetic phase transition with vanishing relaxation rate. Predictions are quantitatively compared with experimental results. The quasielastic peak is typical of a Fermi liquid while the other mode breaks the Fermi liquid description. Our approach might offer new prospects for the study of the quantum critical phenomena in the vicinity of the antiferromagnetic phase transition.

II. PRESENTATION OF THE APPROACH

We consider the Kondo lattice model (KLM) constituted by a periodic array of Kondo impurities with an average number of conduction electrons per site $n_c < 1$. In the grand canonical ensemble, the hamiltonian is written as

$$H = \sum_{k\sigma} \epsilon_k c_{k\sigma}^\dagger c_{k\sigma} + J \sum_i \mathbf{S}_i \cdot \sum_{\sigma\sigma'} c_{i\sigma}^\dagger \boldsymbol{\tau}_{\sigma\sigma'} c_{i\sigma'} - \mu N_S \left(\frac{1}{N_S} \sum_{k\sigma} c_{k\sigma}^\dagger c_{k\sigma} - n_c \right) \quad (1)$$

in which \mathbf{S}_i represents the spin ($S = 1/2$) of the impurities distributed on the sites (in number N_S) of a periodic lattice; $c_{k\sigma}^\dagger$ is the creation operator of the conduction electron of momentum \mathbf{k} , spin quantum number σ characterized by the energy $\epsilon_k = - \sum_{\langle i,j \rangle} t_{ij} \exp(i\mathbf{k} \cdot \mathbf{R}_{ij})$ and the chemical potential μ ; $\boldsymbol{\tau}$ are the Pauli matrices ($\boldsymbol{\tau}^x, \boldsymbol{\tau}^y, \boldsymbol{\tau}^z$) and $\boldsymbol{\tau}^0$ the unit matrix; J is the antiferromagnetic Kondo interaction ($J > 0$).

We use the Abrikosov pseudo-fermion representation of the spin \mathbf{S}_i : $\mathbf{S}_i = \sum_{\sigma\sigma'} f_{i\sigma}^\dagger \boldsymbol{\tau}_{\sigma\sigma'} f_{i\sigma'}$. The projection into the physical subspace is implemented by a local constraint

$$Q_i = \frac{1}{N_S} \sum_{i\sigma} f_{i\sigma}^+ f_{i\sigma} - 1 = 0 \quad (2)$$

A Lagrange multiplier λ_i is introduced to enforce the local constraint Q_i . Since $[Q_i, H] = 0$, λ_i is time-independent.

In this representation, the partition function of the KLM can be expressed as a functional integral over the coherent states of the fermion fields

$$Z = \int \mathcal{D}c_{i\sigma} \mathcal{D}f_{i\sigma} d\lambda_i \exp \left[- \int_0^\beta \mathcal{L}(\tau) d\tau \right] \quad (3)$$

where the Lagrangian $\mathcal{L}(\tau)$ is given by

$$\mathcal{L}(\tau) = \mathcal{L}_0(\tau) + H_0(\tau) + H_J(\tau)$$

$$\mathcal{L}_0(\tau) = \sum_{i\sigma} c_{i\sigma}^\dagger \partial_\tau c_{i\sigma} + f_{i\sigma}^\dagger \partial_\tau f_{i\sigma}$$

$$H_0(\tau) = \sum_{k\sigma} \epsilon_k c_{k\sigma}^\dagger c_{k\sigma} - \mu N_S \left(\frac{1}{N_S} \sum_{k\sigma} c_{k\sigma}^\dagger c_{k\sigma} - n_c \right) + \sum_i \lambda_i Q_i$$

$$H_J(\tau) = J \sum_i \mathbf{S}_{fi} \cdot \mathbf{S}_{ci}$$

with $\mathbf{S}_{c_i} = \sum_{\sigma\sigma'} c_{i\sigma}^\dagger \boldsymbol{\tau}_{\sigma\sigma'} c_{i\sigma'}$ and $\mathbf{S}_{fi} = \mathbf{S}_i$

We perform a Hubbard-Stratonovich transformation on the Kondo interaction term $H_J(\tau)$. Since more than one field is implied in the transformation, an uncertainty is left on the way of decoupling. We propose to remove it in the following way. First, we note that $H_J(\tau)$ may also be written as

$$H_J(\tau) = -\frac{3J}{8} \sum_i n_{fc_i} n_{cf_i} + \frac{J}{2} \sum_i \mathbf{S}_{fc_i} \cdot \mathbf{S}_{cf_i} \quad (4)$$

where $\mathbf{S}_{fc_i} = \sum_{\sigma\sigma'} f_{i\sigma}^\dagger \boldsymbol{\tau}_{\sigma\sigma'} c_{i\sigma'}$ and $n_{fc_i} = \sum_{\sigma\sigma'} f_{i\sigma}^\dagger \tau_{\sigma\sigma'}^0 c_{i\sigma'}$ (respectively \mathbf{S}_{cf_i} and n_{cf_i} their hermitian conjugate).

The Kondo interaction term is then given by any linear combination of $J \sum_i \mathbf{S}_{fi} \cdot \mathbf{S}_{ci}$ (with a weighting factor x) and of the term appearing in the right-hand side of Equation (4) (with a weighting factor $(1-x)$). x is chosen so as to recover the usual results obtained within the slave-boson theories. One can check that this is the case for $x = 1/3$. The Kondo interaction term is then given by

$$H_J(\tau) = J_S \sum_i (\mathbf{S}_{fi} \cdot \mathbf{S}_{ci} + \mathbf{S}_{fc_i} \cdot \mathbf{S}_{cf_i}) - J_C \sum_i n_{fc_i} n_{cf_i} \quad (5)$$

with $J_S = J/4$ and $J_C = J/3$.

Performing a generalized Hubbard-Stratonovich transformation on the partition function Z makes the fields Φ_i, Φ_i^* (for charge) and $\boldsymbol{\xi}_{fi}, \boldsymbol{\xi}_{ci}$ appear (omitting the fields associated to $\mathbf{S}_{fc_i}, \mathbf{S}_{cf_i}$). We get

$$Z = \int d\Phi_i d\Phi_i^* d\boldsymbol{\xi}_{fi} d\boldsymbol{\xi}_{ci} \mathcal{D}c_{i\sigma} \mathcal{D}f_{i\sigma} d\lambda_i \exp \left[- \int_0^\beta \mathcal{L}'(\tau) d\tau \right] \quad (6)$$

with

$$\mathcal{L}'(\tau) = \mathcal{L}_0(\tau) + H_0(\tau) + H'_J(\tau)$$

$$H'_J(\tau) = \sum_{i\sigma\sigma'} \begin{pmatrix} c_{i\sigma}^\dagger & f_{i\sigma}^\dagger \end{pmatrix} \begin{pmatrix} -J_S i \boldsymbol{\xi}_{fi} \cdot \boldsymbol{\tau}_{\sigma\sigma'} & J_C \Phi_i^* \tau_{\sigma\sigma'}^0 \\ J_C \Phi_i \tau_{\sigma\sigma'}^0 & -J_S i \boldsymbol{\xi}_{ci} \cdot \boldsymbol{\tau}_{\sigma\sigma'} \end{pmatrix} \begin{pmatrix} c_{i\sigma'} \\ f_{i\sigma'} \end{pmatrix} + J_C \sum_i \Phi_i^* \Phi_i + J_S \sum_i \boldsymbol{\xi}_{fi} \cdot \boldsymbol{\xi}_{ci}$$

A. Saddle-Point

The saddle-point solution is obtained for space and time independent fields $\Phi_0, \lambda_0, \xi_{f_0}$ and ξ_{c_0} . In the magnetically-disordered regime ($\xi_{f_0} = \xi_{c_0} = 0$), it leads to renormalized bands α and β as schematized in Figure 1. Noting $\sigma_0^{(*)} = J_C \Phi_0^{(*)}$ and $\varepsilon_f = \lambda_0$, $\alpha_{k\sigma}^\dagger |0\rangle$ and $\beta_{k\sigma}^\dagger |0\rangle$ are the eigenstates of

$$\mathbf{G}_0^{-1\sigma}(\mathbf{k}, \tau) = \begin{pmatrix} \partial_\tau + \varepsilon_k & \sigma_0^* \\ \sigma_0 & \partial_\tau + \varepsilon_f \end{pmatrix} \quad (7)$$

with respectively the eigenenergies $(\partial_\tau + E_k^-)$ and $(\partial_\tau + E_k^+)$. In the notations: $x_k = \varepsilon_k - \varepsilon_f$, $y_k^\pm = E_k^\pm - \varepsilon_f$ and $\Delta_k = \sqrt{x_k^2 + 4\sigma_0^2}$, we get

$$y_k^\pm = (x_k \pm \Delta_k) / 2 \quad (8)$$

Let us note $U_{k\sigma}^\dagger$ the matrix transforming the initial basis $(c_{k\sigma}^\dagger, f_{k\sigma}^\dagger)$ to the eigenbasis $(\alpha_{k\sigma}^\dagger, \beta_{k\sigma}^\dagger)$. The hamiltonian being hermitian, the matrix $U_{k\sigma}$ is unitary : $U_{k\sigma} U_{k\sigma}^\dagger = U_{k\sigma}^\dagger U_{k\sigma} = 1$. In the notation $U_{k\sigma}^\dagger = \begin{pmatrix} -v_k & u_k \\ u_k & v_k \end{pmatrix}$, we have

$$u_k = \frac{-\sigma_0 / y_k^-}{\sqrt{1 + (\sigma_0 / y_k^-)^2}} = \frac{1}{2} \left[1 + \frac{x_k}{\Delta_k} \right] \quad (9)$$

$$v_k = \frac{1}{\sqrt{1 + (\sigma_0 / y_k^-)^2}} = \frac{1}{2} \left[1 - \frac{x_k}{\Delta_k} \right]$$

The saddle-point equations together with the conservation of the number of conduction electrons are written as

$$\sigma_0 = \frac{1}{N_S} J_C \sum_{k\sigma} u_k v_k n_F(E_k^-) \quad (10)$$

$$1 = \frac{1}{N_S} \sum_{k\sigma} u_k^2 n_F(E_k^-)$$

$$n_c = \frac{1}{N_S} \sum_{k\sigma} v_k^2 n_F(E_k^-)$$

Their resolution leads to

$$|y_F| = D \exp[-2/(\rho_0 J_C)] \quad (11)$$

$$2\rho_0 \sigma_0^2 / |y_F| = 1$$

$$\mu = 0$$

where $y_F = \mu - \varepsilon_F$ and ρ_0 is the bare density of states of conduction electrons ($\rho_0 = 1/2D$ for a flat band). Noting $y = E - \varepsilon_F$, the density of states at the energy E is $\rho(E) = \rho_0 (1 + \sigma_0^2 / y^2)$. If $n_c < 1$, the chemical potential is located just below the upper edge of the α -band. The system is metallic. The density of states at the Fermi level is strongly enhanced towards the bare density of states of conduction electrons : $\rho(E_F) / \rho_0 = (1 + \sigma_0^2 / y_F^2) \sim 1 / (2\rho_0 |y_F|)$. That corresponds to the flat part of the α -band in Figure 1. It is associated to the formation of a Kondo or Abrikosov-Suhl resonance pinned at the Fermi level resulting of the Kondo effect. The low-lying excitations are quasiparticles of large effective mass m^* as observed in heavy-Fermion systems. Also note the presence of a hybridization gap between the α and the β bands. The direct gap of value $2\sigma_0$ is much larger than the indirect gap equal to $2|y_F|$. The saddle-point solution transposes to $N=2$ the large- N results obtained within the slave-boson mean-field theories (SBMFT).

B. Gaussian fluctuations

We now consider the gaussian fluctuations around the saddle-point solution. Following Read and Newns [17], we take advantage of the local U(1) gauge transformation of the lagrangian $\mathcal{L}'(\tau)$

$$\Phi_i \rightarrow r_i \exp(i\theta_i)$$

$$f_i \rightarrow f'_i \exp(i\theta_i)$$

$$\lambda_i \rightarrow \lambda'_i + i \partial\theta_i/\partial\tau$$

We use the radial gauge in which the modulus of both fields Φ_i and Φ_i^* are the radial field r_i , and their phase θ_i (via its time derivative) is incorporated into the Lagrange multiplier λ_i which turns out to be a field. Use of the radial instead of the cartesian gauge bypasses the familiar complications of infrared divergences associated with unphysical Goldstone bosons. We let the fields fluctuate away from their saddle-point values : $r_i = r_0 + \delta r_i$, $\lambda_i = \lambda_0 + \delta\lambda_i$, $\xi_{f_i} = \delta\xi_{f_i}$ and $\xi_{c_i} = \delta\xi_{c_i}$. After integrating out the Grassmann variables in the partition function in Equation (6), we get

$$Z = \int \mathcal{D}r_i \mathcal{D}\lambda_i \mathcal{D}\xi_{f_i} \mathcal{D}\xi_{c_i} \exp[-S_{eff}] \quad (12)$$

where the effective action is

$$S_{eff} = - \sum_{k, i\omega_n} Ln Det \mathbf{G}^{-1}(\mathbf{k}, i\omega_n) + \beta [J_C \sum_i r_i^2 + J_S \sum_i \xi_{f_i} \cdot \xi_{c_i} + N_S(\mu n_c - \lambda_0)]$$

with :

$$[\mathbf{G}^{-1}(i\omega_n)]_{ij}^{\sigma\sigma'} = \begin{pmatrix} [(-i\omega_n - \mu)\delta_{ij} - t_{ij}]\delta_{\sigma\sigma'} - J_S i \xi_{f_i} \cdot \boldsymbol{\tau}_{\sigma\sigma'} \delta_{ij} & (\sigma_0 + J_C \delta r_i) \delta_{\sigma\sigma'} \delta_{ij} \\ (\sigma_0 + J_C \delta r_i) \delta_{\sigma\sigma'} \delta_{ij} & [-i\omega_n + \varepsilon_f + \delta\lambda_i] \delta_{\sigma\sigma'} \delta_{ij} - J_S i \xi_{c_i} \cdot \boldsymbol{\tau}_{\sigma\sigma'} \delta_{ij} \end{pmatrix}$$

Expanding up to the second order in the Bose fields, one obtains the gaussian corrections $S_{eff}^{(2)}$ to the saddle-point effective action

$$S_{eff}^{(2)} = \frac{1}{\beta} \sum_{\mathbf{q}, i\omega_\nu} [(\delta r \ \delta\lambda) \mathbf{D}_C^{-1}(\mathbf{q}, i\omega_\nu) \begin{pmatrix} \delta r \\ \delta\lambda \end{pmatrix} + (\delta\xi_f^z \ \delta\xi_c^z) \mathbf{D}_S^{\parallel-1}(\mathbf{q}, i\omega_\nu) \begin{pmatrix} \delta\xi_f^z \\ \delta\xi_c^z \end{pmatrix} \\ + (\delta\xi_f^+ \ \delta\xi_c^+) \mathbf{D}_S^{\perp-1}(\mathbf{q}, i\omega_\nu) \begin{pmatrix} \delta\xi_f^+ \\ \delta\xi_c^+ \end{pmatrix} + (\delta\xi_f^- \ \delta\xi_c^-) \mathbf{D}_S^{\perp-1}(\mathbf{q}, i\omega_\nu) \begin{pmatrix} \delta\xi_f^- \\ \delta\xi_c^- \end{pmatrix}] \quad (13)$$

where the boson propagators split into the following charge and longitudinal spin parts

$$\mathbf{D}_C^{-1}(\mathbf{q}, i\omega_\nu) = \begin{pmatrix} J_C[1 - J_C(\bar{\varphi}_2(\mathbf{q}, i\omega_\nu) + \bar{\varphi}_m(\mathbf{q}, i\omega_\nu))] & -J_C \bar{\varphi}_1(\mathbf{q}, i\omega_\nu) \\ -J_C \bar{\varphi}_1(\mathbf{q}, i\omega_\nu) & -\bar{\varphi}_{ff}(\mathbf{q}, i\omega_\nu) \end{pmatrix} \quad (14)$$

$$\mathbf{D}_S^{\parallel-1}(\mathbf{q}, i\omega_\nu) = \begin{pmatrix} J_S^2 \varphi_{ff}^{\parallel}(\mathbf{q}, i\omega_\nu) & J_S[1 + J_S \varphi_{cf}^{\parallel}(\mathbf{q}, i\omega_\nu)] \\ J_S[1 + J_S \varphi_{fc}^{\parallel}(\mathbf{q}, i\omega_\nu)] & J_S^2 \varphi_{cc}^{\parallel}(\mathbf{q}, i\omega_\nu) \end{pmatrix}$$

and equivalent expression for the transverse spin part $\mathbf{D}_S^{\perp-1}(\mathbf{q}, i\omega_\nu)$. The expression of the different bubbles are given in the appendix. The charge boson propagator $\mathbf{D}_C(\mathbf{q}, i\omega_\nu)$ associated to the Kondo effect is equivalent to that obtained in the $1/N$ expansion theories. The originality of the approach is to simultaneously derive the spin propagator $\mathbf{D}_S^{\parallel-1}(\mathbf{q}, i\omega_\nu)$ and $\mathbf{D}_S^{\perp-1}(\mathbf{q}, i\omega_\nu)$ associated to the spin fluctuation effects. Note that in the magnetically-disordered phase, the charge and spin contributions in S_{eff} are totally decoupled.

III. DYNAMICAL SPIN SUSCEPTIBILITY

Next step is to consider the dynamical spin susceptibility. For that purpose, we study the linear response M_f to the source-term $-2\mathbf{S}_f \cdot \mathbf{B}$ (we consider \mathbf{B} colinear to the \mathbf{z} -axis). The effect on the partition function expressed in Equation (6) is to change the hamiltonian $H'_J(\tau)$ to $H'^B_J(\tau)$

$$H'^B_J(\tau) = \sum_{i\sigma\sigma'} (c_{i\sigma}^\dagger \ f_{i\sigma}^\dagger) \left(\begin{array}{c} -J_S i \boldsymbol{\xi}_{f_i} \cdot \boldsymbol{\tau}_{\sigma\sigma'} \\ J_C \Phi_i \tau_{\sigma\sigma'}^0 \\ \sum_{\alpha=x,y,z} (-J_S i \xi_{c_i}^\alpha - B \delta_{\alpha z}) \cdot \tau_{\sigma\sigma'}^\alpha \end{array} \right) \begin{pmatrix} c_{i\sigma'} \\ f_{i\sigma'} \end{pmatrix} + J_C \sum_i \Phi_i^* \Phi_i + J_S \sum_i \boldsymbol{\xi}_{f_i} \cdot \boldsymbol{\xi}_{c_i} \quad (15)$$

Introducing the change of variables $\xi_{c_i}^\alpha = \xi_{c_i}^\alpha - iB/J_S$, we connect the f magnetization and the ff dynamical spin susceptibility to the Hubbard Stratonovich fields $\boldsymbol{\xi}_{f_i}$

$$M_f^z = -\frac{1}{\beta} \frac{\partial \ln Z}{\partial B_z} = i \langle \xi_{f_i}^z \rangle$$

$$\chi_{ff}^{\alpha\beta} = -\frac{1}{\beta} \frac{\partial^2 \ln Z}{\partial B^\alpha \partial B^\beta} = -\langle \xi_{f_i}^\alpha \xi_{f_i}^\beta \rangle + \langle \xi_{f_i}^\alpha \rangle \langle \xi_{f_i}^\beta \rangle \quad (16)$$

Using the expression (14) for the boson propagator $\mathbf{D}_S^{\parallel -1}(\mathbf{q})$, we get for the longitudinal spin susceptibility

$$\chi_{ff}^{\parallel}(\mathbf{q}, i\omega_\nu) = \frac{\varphi_{ff}^{\parallel}(\mathbf{q}, i\omega_\nu)}{1 - J_S^2 [\varphi_{ff}^{\parallel}(\mathbf{q}, i\omega_\nu) \varphi_{cc}^{\parallel}(\mathbf{q}, i\omega_\nu) - \varphi_{fc}^{\parallel 2}(\mathbf{q}, i\omega_\nu) - \frac{2}{J_S} \varphi_{fc}^{\parallel}(\mathbf{q}, i\omega_\nu)]} \quad (17)$$

and equivalent expression for the transverse spin susceptibility $\chi_{ff}^\perp(\mathbf{q}, i\omega_\nu)$. The diagrammatic representation of Equation (17) is reported in Figure 2. The different bubbles $\varphi_{ff}^{\parallel}(\mathbf{q}, i\omega_\nu)$, $\varphi_{cc}^{\parallel}(\mathbf{q}, i\omega_\nu)$ and $\varphi_{fc}^{\parallel}(\mathbf{q}, i\omega_\nu)$ are evaluated from the expressions of the Green's functions

$$G_{ff}(\mathbf{k}, i\omega_n) = u_k^2 G_{\alpha\alpha}(\mathbf{k}, i\omega_n) + v_k^2 G_{\beta\beta}(\mathbf{k}, i\omega_n) \quad (18)$$

$$G_{cc}(\mathbf{k}, i\omega_n) = v_k^2 G_{\alpha\alpha}(\mathbf{k}, i\omega_n) + u_k^2 G_{\beta\beta}(\mathbf{k}, i\omega_n)$$

$$G_{cf}(\mathbf{k}, i\omega_n) = G_{fc}(\mathbf{k}, i\omega_n) = -u_k v_k [G_{\alpha\alpha}(\mathbf{k}, i\omega_n) - G_{\beta\beta}(\mathbf{k}, i\omega_n)]$$

where $G_{\alpha\alpha}(\mathbf{k}, i\omega_n)$ and $G_{\beta\beta}(\mathbf{k}, i\omega_n)$ are the Green's functions associated to the eigenstates $\alpha_{k\sigma}^\dagger |0\rangle$ and $\beta_{k\sigma}^\dagger |0\rangle$. In the low frequency limit, one can easily check that the dynamical spin susceptibility may be written as

$$\chi_{ff}(\mathbf{q}, i\omega_\nu) = \frac{\chi_{\alpha\alpha}(\mathbf{q}, i\omega_\nu) + \bar{\chi}_{\alpha\beta}(\mathbf{q}, i\omega_\nu)}{1 - J_S^2 \chi_{\alpha\alpha}(\mathbf{q}, i\omega_\nu) \bar{\chi}_{\alpha\beta}(\mathbf{q}, i\omega_\nu)} \quad (19)$$

for both the longitudinal and the transverse parts.

$$\chi_{\alpha\alpha}(\mathbf{q}, i\omega_\nu) = \frac{1}{\beta} \sum_k \frac{n_F(E_k^-) - n_F(E_{k+q}^-)}{i\omega_\nu - E_{k+q}^- + E_k^-}$$

$$\bar{\chi}_{\alpha\beta}(\mathbf{q}, i\omega_\nu) = \frac{1}{\beta} \sum_k (u_k^2 v_{k+q}^2 + v_k^2 u_{k+q}^2) \frac{n_F(E_k^-) - n_F(E_{k+q}^+)}{i\omega_\nu - E_{k+q}^+ + E_k^-}$$

Equation (19) constitutes the main result of the paper from which the whole physical discussion on the \mathbf{q} - and ω - dependence of the dynamical spin susceptibility follows and comparison with experiments is made.

IV. PHYSICAL DISCUSSION

From Equation (19), one can see that the dynamical spin susceptibility is made of two contributions $\chi_{intra}(\mathbf{q}, i\omega_\nu)$ and $\chi_{inter}(\mathbf{q}, i\omega_\nu)$

$$\chi_{ff}(\mathbf{q}, i\omega_\nu) = \chi_{intra}(\mathbf{q}, i\omega_\nu) + \chi_{inter}(\mathbf{q}, i\omega_\nu) \quad (20)$$

with

$$\chi_{intra}(\mathbf{q}, i\omega_\nu) = \frac{\chi_{\alpha\alpha}(\mathbf{q}, i\omega_\nu)}{1 - J_S^2 \chi_{\alpha\alpha}(\mathbf{q}, i\omega_\nu) \bar{\chi}_{\alpha\beta}(\mathbf{q}, i\omega_\nu)} \quad (21)$$

$$\chi_{inter}(\mathbf{q}, i\omega_\nu) = \frac{\bar{\chi}_{\alpha\beta}(\mathbf{q}, i\omega_\nu)}{1 - J_S^2 \chi_{\alpha\alpha}(\mathbf{q}, i\omega_\nu) \bar{\chi}_{\alpha\beta}(\mathbf{q}, i\omega_\nu)} \quad (22)$$

$\chi_{intra}(\mathbf{q}, i\omega_\nu)$ and $\chi_{inter}(\mathbf{q}, i\omega_\nu)$ respectively represent the renormalized particle-hole pair excitations within the lower α band, and from the lower α to the upper β band. The latter expression is reminiscent of the behaviour proposed by Bernhoeft and Lonzarich [7] to explain the neutron scattering observed in UPt_3 with the existence of both a "slow" and a "fast" component in $\chi''(\mathbf{q}, \omega)/\omega$ due to spin-orbit coupling. Also in a phenomenological way, the same type of feature has been suggested in the duality model developed by Kuramoto and Miyake [27]. To our knowledge, the proposed approach provides the first microscopic derivation from the Kondo lattice model of such a behaviour. The bare intraband susceptibility $\chi_{\alpha\alpha}(\mathbf{q}, \omega)$ is well approximated by a lorentzian

$$\chi_{\alpha\alpha}^{-1}(\mathbf{q}, \omega) = \rho_{\alpha\alpha}(\mathbf{q})^{-1} \left(1 - i \frac{\omega}{\Gamma_0(\mathbf{q})} \right) \quad (23)$$

where $\rho_{\alpha\alpha} = \chi'_{\alpha\alpha}(\mathbf{q}, 0)$ and $\Gamma_0(\mathbf{q})$ is the relaxation rate of order $|y_F| = T_K$. This corresponds to the Lindhard continuum of the intraband particle-hole pair excitations $\chi''_{\alpha\alpha}(\mathbf{q}, \omega) \neq 0$ as reported in Figure 3. In the same way, we propose to schematize the low-frequency behavior ($\omega \ll \omega_0(\mathbf{q})$) of the bare interband susceptibility by

$$\bar{\chi}'_{\alpha\beta}{}^{-1}(\mathbf{q}, \omega) = \rho_{\alpha\beta}(\mathbf{q})^{-1} \left(1 - \frac{\omega}{\omega_0(\mathbf{q})} \right) \quad (24)$$

where $\rho_{\alpha\beta} = \bar{\chi}'_{\alpha\beta}(\mathbf{q}, 0)$ and $\omega_0(\mathbf{q})$ is a characteristic frequency-scale of the interband transitions. The value of $\omega_0(\mathbf{q})$ is strongly structure-dependent. In the simple case of a cubic band structure $\epsilon_k = -2t(\cos k_x + \cos k_y + \cos k_z)$ (tight-binding scheme including nearest-neighbor hopping), we find a weakly wavevector dependent frequency around $\mathbf{q} = \mathbf{Q}$ of order of $\omega_0 = 2|y_F| / (\rho_0 J_C)$. The latter result does not stand for more complicated band structures as obtained by de Haas-van Alphen studies [29] combined with band structure calculations in heavy-Fermion compounds. In the following, we will leave $\omega_0(\mathbf{q})$ as a parameter. Figure 3 reports the continuum of interband particle-hole excitations $\bar{\chi}_{\alpha\beta}'' \neq 0$. Due to the presence of the hybridization gap in the density of states, the latter continuum displays a gap equal to $2\sigma_0$, the value of the direct gap at $\mathbf{q} = \mathbf{0}$, and $2|y_F|$, the value of the indirect gap at $\mathbf{q} = \mathbf{Q}$ (close to k_F). More precisely, we have shown

$$\bar{\chi}_{\alpha\beta}''(\mathbf{0}, \omega) = 4\rho_0 \frac{\sigma_0^2}{\omega \sqrt{\omega^2 - 4\sigma_0^2}} \text{ at } 2\sigma_0 < \omega < D \quad (25)$$

$$\bar{\chi}_{\alpha\beta}''(\mathbf{Q}, \omega) = 2\rho_0 \frac{1}{1 + \omega^2 / (2\sigma_0)^2} \text{ at } 2|y_F| < \omega < 2D$$

Far from the antiferromagnetic wavevector $\mathbf{Q} = (\pi, \pi, \pi)$, $\chi_{ff}(\mathbf{q}, \omega)$ is dominated by the intraband transitions. In the low frequency limit, the frequency dependence of $\chi_{intra}(\mathbf{q}, \omega)$ can be approximate to a lorentzian

$$\chi_{ff}''(\mathbf{q}, \omega) \approx \chi_{intra}''(\mathbf{q}, \omega) = \omega \frac{\chi'_{intra}(\mathbf{q}) \Gamma_{intra}(\mathbf{q})}{\omega^2 + \Gamma_{intra}(\mathbf{q})^2} \quad (26)$$

with

$$\Gamma_{intra}(\mathbf{q}) = \Gamma_0(\mathbf{q})(1 - I(\mathbf{q})) \quad (27)$$

$$\chi'_{intra}(\mathbf{q}) = \frac{\rho_{\alpha\alpha}(\mathbf{q})}{(1 - I(\mathbf{q}))}$$

$I(\mathbf{q}) = J_S^2 \chi'_{\alpha\alpha}(\mathbf{q}, 0) \bar{\chi}'_{\alpha\beta}(\mathbf{q}, 0)$. One has: $\chi'_{\alpha\alpha}(\mathbf{0}, 0) = \rho_{\alpha\alpha}(\mathbf{0}) = \rho(E_F)$ and $\chi'_{\alpha\beta}(\mathbf{0}, 0) = \rho_0$. The contribution expressed in equation (26) is consistent with the standard Fermi liquid theory. Note that the product $\Gamma_{intra}(\mathbf{q})\chi'_{intra}(\mathbf{q}) = \rho_{\alpha\alpha}(\mathbf{q})\Gamma_0(\mathbf{q})$ is independent of I .

Oppositely, at the antiferromagnetic wavevector \mathbf{Q} , $\chi_{ff}(\mathbf{q}, \omega)$ is driven by the interband contribution and we get

$$\chi''_{ff}(\mathbf{Q}, \omega) \approx \chi''_{inter}(\mathbf{Q}, \omega) = \omega \frac{I\chi'_{inter}\Gamma_{inter}}{(\omega - \omega_{\max})^2 + \Gamma_{inter}^2} \quad (28)$$

with

$$\omega_{\max} = \omega_0(1 - I) \quad (29)$$

$$\Gamma_{inter} = \omega_0^2(1 - I)/\Gamma_0$$

$$\chi'_{inter} = \rho_{\alpha\beta}/(1 - I)$$

where ω_0 , $\rho_{\alpha\beta}$, Γ_0 and I are the values of $\omega_0(\mathbf{q})$, $\rho_{\alpha\beta}(\mathbf{q})$ and $\Gamma_0(\mathbf{q})$ and $I(\mathbf{q})$ at $\mathbf{q} = \mathbf{Q}$. The role of the interband transitions have already been pointed out in previous works [21]. However while the previous studies conclude to the presence of an inelastic peak at finite value of the frequency related to the hybridization gap whatever the interaction J is, we emphasize that the renormalization of $\bar{\chi}_{\alpha\beta}(\mathbf{Q}, \omega)$ into $\chi_{inter}(\mathbf{Q}, \omega)$ leads to a noteworthy renormalization of the interband gap. Due to the damping introduced by intraband transitions, $\chi''_{inter}(\mathbf{Q}, \omega)$ takes a finite value at frequency much smaller than the hybridization gap. Both the relaxation rate Γ_{inter} vanishes and the susceptibility χ'_{inter} diverges at the antiferromagnetic transition with again the product $\Gamma_{inter}\chi'_{inter}$ independent of I . Remarkably, the value ω_{\max} of the maximum of $\chi''_{inter}(\mathbf{Q}, \omega)/\omega$ is at the same time pushed to zero. Such a behaviour has been effectively observed in $Ce_{1-x}La_xRu_2Si_2$ [8] with a reduction of Γ_{inter} and ω_{\max} respectively by a factor 4 and 6 when x goes from 0 to 0.075 so when getting closer to the magnetic instability occurring at $x = 0.08$. In order to make the comparison more quantitative, we propose to deduce the values of ω_0 and $(1 - I)$ from the experimental data using the equations (29): $\omega_0 = \Gamma_0\Gamma_{inter}/\omega_{\max}$ and $(1 - I) = \omega_{\max}^2/(\Gamma_0\Gamma_{inter})$. Table II reports the results starting from the experimental values of $\Gamma_0, \Gamma_{inter}, \omega_{\max}$ (respectively noted $\Gamma_{SS}, \Gamma_{IS}, \omega_0$ in experimental papers) extracted from the INS results obtained in $CeCu_6$ (ref. [3]) and $Ce_{1-x}La_xRu_2Si_2$ at $x = 0$ and $x = 0.075$ (ref. [8]). The predictions for ω_0 and $(1 - I)$ in these compounds seem reasonable. The Stoner enhancement factor $(1 - I)$ decreases in $Ce_{1-x}La_xRu_2Si_2$ from $x = 0$ to $x = 0.075$. $(1 - I)$ of $CeCu_6$ is intermediate between those two systems.

V. CONCLUSION

In this paper, we have set up a new approach of the $S = 1/2$ Kondo lattice model which enlarges the standard $1/N$ expansion theories up on the spin fluctuation effects. The latter effects are proved to be essential for the behaviour of the dynamical spin susceptibility near the magnetic phase transition. Our approach provides a microscopic derivation of the main features assumed in the phenomenological models of heavy Fermions as the duality model. We predict a two-component behaviour of the dynamical spin susceptibility: a quasielastic peak typical of the Fermi liquid excitations, and an inelastic peak at a value ω_{\max} of the frequency which is strongly renormalized due to spin fluctuation effects. Outstandingly well, the frequency of the inelastic peak is pushed to zero at the antiferromagnetic transition at the same time as the frequency width vanishes. The results have been compared to the Inelastic Neutron Scattering experiment data with reasonable predictions for

the Stoner enhancement factor $(1 - I)$ and the characteristic frequency ω_0 of the interband contribution to the susceptibility. Obviously, more experiments are needed for a systematic test. The issue is important since it may have implications for the quantum critical phenomena around the antiferromagnetic critical point. Work is currently in progress in that direction and will be presented in a forthcoming paper. We expect the two underlined modes to have different effects on the critical behaviour with, on the one hand, the first "intra-band" mode acting as a paramagnon mode as in the Hertz-Moriya-Millis theory [5], and on the other hand, additional effects brought by the second "inter-band" mode.

ACKNOWLEDGEMENTS

We would like to thank G.G. Lonzarich, N.R. Bernhoeft, G.J. McMullan, L.P. Regnault, J. Flouquet, S. Raymond, P. Brison and K. Miyake for very helpful discussions.

APPENDIX

The expressions of the different bubbles appearing in the expression of the boson propagators (cf. Eq.14) are given here (with $i=1, 2, m$ or ff)

$$\begin{aligned} \overline{\varphi}_i(\mathbf{q}, i\omega_\nu) &= \varphi_i(\mathbf{q}, i\omega_\nu) + \varphi_i(-\mathbf{q}, -i\omega_\nu) \tag{30} \\ \varphi_1(\mathbf{q}, i\omega_\nu) &= -\frac{1}{\beta} \sum_{k\sigma, i\omega_n} G_{cf_0}^\sigma(\mathbf{k} + \mathbf{q}, i\omega_n + i\omega_\nu) G_{ff_0}^\sigma(\mathbf{k}, i\omega_n) \\ \varphi_2(\mathbf{q}, i\omega_\nu) &= -\frac{1}{\beta} \sum_{k\sigma, i\omega_n} G_{cc_0}^\sigma(\mathbf{k} + \mathbf{q}, i\omega_n + i\omega_\nu) G_{ff_0}^\sigma(\mathbf{k}, i\omega_n) \\ \varphi_m(\mathbf{q}, i\omega_\nu) &= -\frac{1}{\beta} \sum_{k\sigma, i\omega_n} G_{cf_0}^\sigma(\mathbf{k} + \mathbf{q}, i\omega_n + i\omega_\nu) G_{cf_0}^\sigma(\mathbf{k}, i\omega_n) \\ \varphi_{ff}^\parallel(\mathbf{q}, i\omega_\nu) &= -\frac{1}{\beta} \sum_{k\sigma, i\omega_n} G_{ff_0}^\sigma(\mathbf{k} + \mathbf{q}, i\omega_n + i\omega_\nu) G_{ff_0}^\sigma(\mathbf{k}, i\omega_n) \\ \varphi_{cc}^\parallel(\mathbf{q}, i\omega_\nu) &= -\frac{1}{\beta} \sum_{k\sigma, i\omega_n} G_{cc_0}^\sigma(\mathbf{k} + \mathbf{q}, i\omega_n + i\omega_\nu) G_{cc_0}^\sigma(\mathbf{k}, i\omega_n) \\ \varphi_{fc}^\parallel(\mathbf{q}, i\omega_\nu) &= -\frac{1}{\beta} \sum_{k\sigma, i\omega_n} G_{fc_0}^\sigma(\mathbf{k} + \mathbf{q}, i\omega_n + i\omega_\nu) G_{fc_0}^\sigma(\mathbf{k}, i\omega_n) \\ \varphi_{ff}^\perp(\mathbf{q}, i\omega_\nu) &= -\frac{1}{\beta} \sum_{k\sigma, i\omega_n} G_{ff_0}^\uparrow(\mathbf{k} + \mathbf{q}, i\omega_n + i\omega_\nu) G_{ff_0}^\downarrow(\mathbf{k}, i\omega_n) \\ \varphi_{cc}^\perp(\mathbf{q}, i\omega_\nu) &= -\frac{1}{\beta} \sum_{k\sigma, i\omega_n} G_{cc_0}^\uparrow(\mathbf{k} + \mathbf{q}, i\omega_n + i\omega_\nu) G_{cc_0}^\downarrow(\mathbf{k}, i\omega_n) \\ \varphi_{fc}^\perp(\mathbf{q}, i\omega_\nu) &= -\frac{1}{\beta} \sum_{k\sigma, i\omega_n} G_{fc_0}^\uparrow(\mathbf{k} + \mathbf{q}, i\omega_n + i\omega_\nu) G_{fc_0}^\downarrow(\mathbf{k}, i\omega_n) \end{aligned}$$

where $G_{cc_0}^\sigma(\mathbf{k}, i\omega_n)$, $G_{ff_0}^\sigma(\mathbf{k}, i\omega_n)$ and $G_{fc_0}^\sigma(\mathbf{k}, i\omega_n)$ are the Green's functions at the saddle-point level obtained by inverting the matrix $G_0^\sigma(\mathbf{k}, \tau)$ defined in Equation (7).

¹ Present Address: Department of Physics, MIT Ma02139 Cambridge, US

² Also Part of the Centre National de la Recherche Scientifique (CNRS)

- [1] H.von Löhneysen, A. Schröder, M. Sieck, T. Trappmann Phys.Rev.Lett. **72**, 3262 (1994); H.von Löhneysen J.Phys.Cond.Matt. **8**, 9689 (1996); O. Stockert, H.v. Löhneysen, A. Schröder, M. Loewenhaupt, N. Pyka, P.L. Gammel, U. Yaron Physica B **230-232**, 247 (1997)
- [2] S. Kambe, S. Raymond, L.P. Regnault, J. Flouquet, P. Lejay, P. Haen J.Phys.Soc.Jpn **65**, 3294 (1996)
- [3] L.P. Regnault, W.A.C. Erkelens, J. Rossat-Mignod, P. Lejay, J. Flouquet Phys. Rev. **B 38**, 4481 (1988); J. Rossat-Mignod, L.P. Regnault, J.L. Jacoud, C. Vettier, P. Lejay, J. Flouquet, E. Walker, D. Jaccard, A. Amato J.Magn.Magn.Mater. **76-77**, 376 (1988)
- [4] G. Aeppli, H. Yoshizawa, Y. Endoh, E. Bucher, J. Hufnagl Phys.Rev.Lett. **57**, 122 (1986); G. Aeppli, A. Goldman, G. Shirane, E. Bucher, M.C. Lux-Steiner Phys.Rev.Lett. **58**, 808 (1987); G. Aeppli, C. Broholm in Handbook on the Physics and Chemistry of Rare Earths (ed. by Gschneidner et al, Elsevier 1994) Vol. 19, p. 123; A. Schröder, G. Aeppli, E. Bucher submitted to Physica B, International Conference on Neutron Scattering, Toronto (1997)
- [5] J.A. Hertz Phys.Rev. B **14**, 1165 (1976); A.J. Millis Phys.Rev. B **48**, 7183 (1993); T. Moriya, T. Takimoto J. Phys. Soc. Jpn **64**, 960 (1995)
- [6] A. Rosch, A. Schröder, O. Stockert, H.v. Löhneysen Phys. Rev. Lett. **79**, 159 (1997); A. Schröder, G. Aeppli, E. Bucher, R. Ramazashvili, P. Coleman cond-mat 9803004
- [7] N.R. Bernhoeft, G.G. Lonzarich J.Phys.Cond.Mat. **7**, 7325 (1995)
- [8] S. Raymond, L.P. Regnault, S. Kambe, J.M. Mignod, P. Lejay, J. Flouquet J.Low Temp.Phys. **109**, 205 (1997)
- [9] H. Tsunetsugu, M. Sigrist, K. Ueda Rev.Mod.Phys. **69**, 809 (1997)
- [10] S. Doniach Physica B **91**, 231 (1977)
- [11] C. Lacroix, M. Cyrot Phys.Rev. B **20**, 1969 (1979)
- [12] B.H. Brandow Phys.Rev. B **33**, 215 (1986)
- [13] P. Fazekas and H. Shiba Intern.J.Mod.Phys. B **5**, 289 (1991)
- [14] T.M. Rice and K. Ueda Phys.Rev.Lett. **55**, 995 (1985)
- [15] A.V. Goltsev Physica B bf 192, 403 (1993)
- [16] P. Coleman Phys.Rev. B **29**, 3035 (1984)
- [17] N. Read, D.N. Newns J.Phys.C **16**, 3273 (1983)
- [18] A.J. Millis, P.A. Lee Phys.Rev. B **35**, 3394 (1987)
- [19] A. Auerbach, K. Levin Phys.Rev.Lett. **57**, 877 (1986)
- [20] M. Lavagna, A.J. Millis, P.A. Lee Phys.Rev.Lett. **58**, 266 (1987)
- [21] A. Auerbach, Ju H. Kim, K. Levin, M.R. Norman Phys. Rev. Lett. **60**, 623 (1988)
- [22] A. Houghton, N. Read, H. Won Phys.Rev. B **37**, 3782 (1988)
- [23] S. Doniach Phys.Rev. B **35**, 1814 (1987)
- [24] C. Lacroix J.Magn.Magn.Mater. **100**, 90 (1991)
- [25] S.M.M. Evans J.Phys.: Condens.Matter **3**, 8441 (1991)
- [26] S.M.M. Evans, B. Coqblin Phys.Rev. B **43**, 12790 (1991)
- [27] Y. Kuramoto, K. Miyake J. Phys.Soc.Jpn **59**, 2831 (1990)
- [28] Y. Kuramoto Solid State Comm. **63**, 467 (1987)
- [29] S.R. Julian, F.S. Tautz, G.J. McMullan, G.G. Lonzarich Physica B **199 – 200**, 63 (1994); M. Takashita, H. Aoki, T. Terashima, S. Uji, K. Maezawa, R. Settai, Y. Onuki J.Phys.Soc.Jpn. **65**, 515 (1996)

TABLE CAPTIONS

Table I: Values of the single-site and intersite relaxation rates Γ_{SS} and Γ_{IS} and position of the inelastic peak ω_{max} extracted from the Inelastic Neutron Scattering (INS) measurements performed in $CeCu_6$ (ref. [3]) and $Ce_{1-x}La_xRu_2Si_2$ at $x = 0$ and $x = 0.075$ (ref. [8]).

Table II: Predicted values of the characteristic frequency-scale ω_0 for the interband transitions and the Stoner enhancement factor $(1 - I)$ from the INS data on Γ_{SS} , Γ_{IS} and ω_0 (respectively noted Γ_0 , Γ_{inter} and ω_{max} in experimental papers) for the same three compounds as in Table I. Note that $Ce_{1-x}La_xRu_2Si_2$ at $x = 0.075$ is very close to the antiferromagnetic instability while the Stoner enhancement factor $(1 - I)$ for $CeCu_6$ is intermediate between that of the two concentrations $x = 0$ and $x = 0.075$ of $Ce_{1-x}La_xRu_2Si_2$.

Table I

| | $\Gamma_{SS}(meV)$ | $\Gamma_{IS}(meV)$ | $\omega_{max}(meV)$ |
|------------------------|--------------------|--------------------|---------------------|
| $CeCu_6$ | 0.42 | 0.2 | 0.25 |
| $CeRu_2Si_2$ | 2.0 | 0.75 | 1.2 |
| $Ce_{1-x}La_xRu_2Si_2$ | 1.4 | 0.2 | 0.2 |

Table II

| | $\Gamma_0(meV)$ | $\Gamma_{inter}(meV)$ | $\omega_{max}(meV)$ | $\omega_0 _{ded.}(meV)$ | $(1 - I) _{ded.}$ |
|------------------------|-----------------|-----------------------|---------------------|-------------------------|-------------------|
| $CeCu_6$ | 0.42 | 0.2 | 0.25 | 0.34 | 0.74 |
| $CeRu_2Si_2$ | 2.0 | 0.75 | 1.2 | 1.25 | 0.96 |
| $Ce_{1-x}La_xRu_2Si_2$ | 1.4 | 0.2 | 0.2 | 1.4 | 0.14 |

FIGURE CAPTIONS

Figure 1: Energy versus wave-vector k for the two bands α and β . Note the presence of a direct gap of value $2\sigma_0$ and of an indirect gap of value $2|y_F|$.

Figure 2: Diagrammatic representation of Equation (25) for the dynamical spin susceptibility $\chi_{ff}(\mathbf{q}, \omega)$.

Figure 3: Continuum of the intra- and interband electron-hole pair excitations $\chi''_{\alpha\alpha}(q, \omega) \neq 0$ and $\chi''_{\alpha\beta}(q, \omega) \neq 0$. Note the presence of a gap in the interband transitions equal to the indirect gap of value $2|y_F|$ at $q = k_F$, and to the direct gap of value $2\sigma_0$ at $q = 0$.

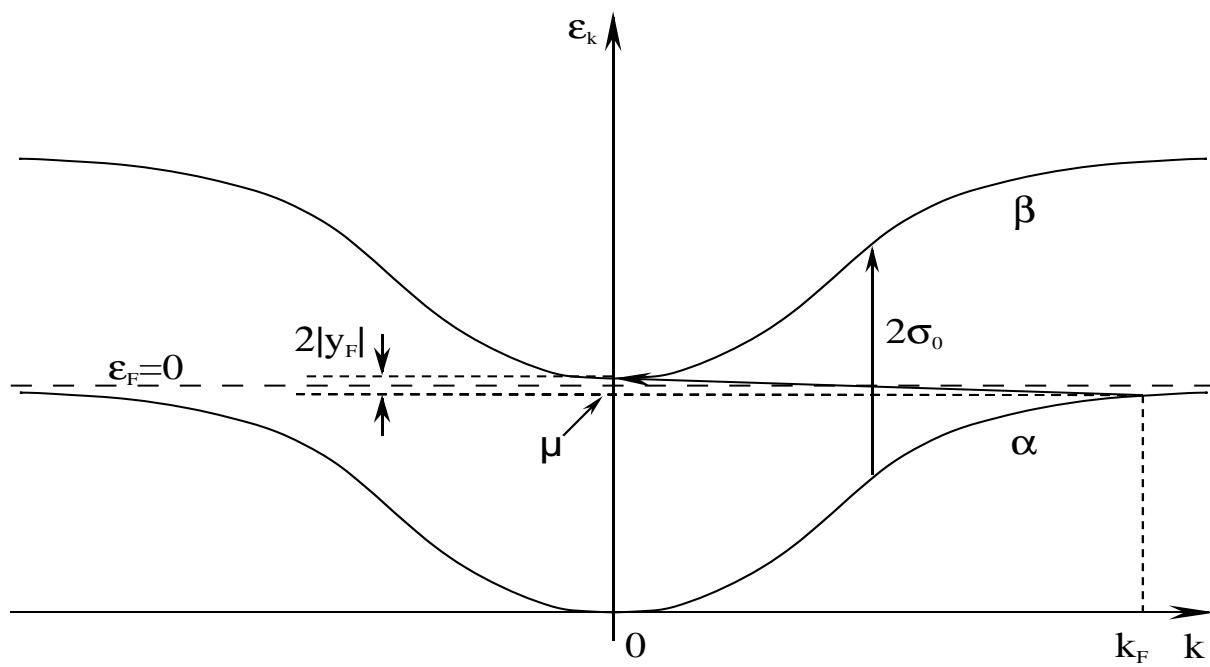


FIG. 1.

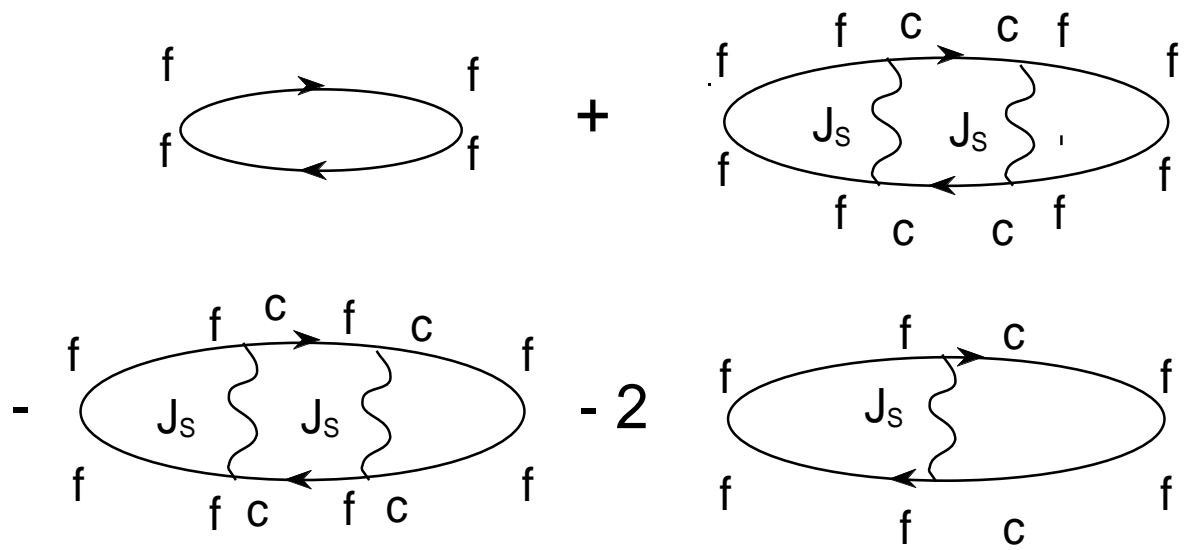


FIG. 2.

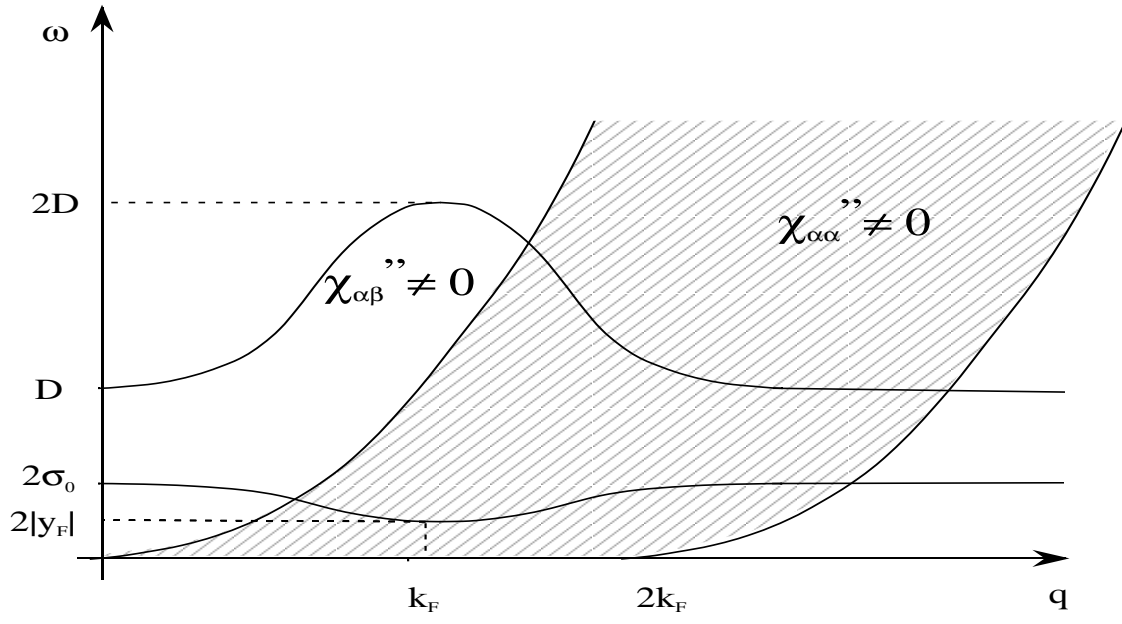


FIG. 3.